

# Verifiable cloud-based variational quantum algorithms

Junhong Yang,<sup>1</sup> Banghai Wang,<sup>1,\*</sup> Junyu Quan,<sup>2</sup> and Qin Li<sup>3,†</sup>

<sup>1</sup>*School of Computer Science and Technology, Guangdong University of Technology, Guangzhou 510006, People's Republic of China*

<sup>2</sup>*School of Mathematics and Computational Science, Xiangtan University, Xiangtan 411105, People's Republic of China*

<sup>3</sup>*School of Computer Science, Xiangtan University, Xiangtan 411105, People's Republic of China*

Variational quantum algorithms (VQAs) have shown potential for quantum advantage with noisy intermediate-scale quantum (NISQ) devices for quantum machine learning (QML). However, given the high cost and limited availability of quantum resources, delegating VQAs via cloud networks is a more practical solution for clients with limited quantum capabilities. Recently, Shingu et al.[Physical Review A, 105, 022603 (2022)] proposed a variational secure cloud quantum computing protocol, utilizing ancilla-driven quantum computation (ADQC) for cloud-based VQAs with minimal quantum resource consumption. However, their protocol lacks verifiability, which exposes it to potential malicious behaviors by the server. Additionally, channel loss requires frequent re-delegation as the size of the delegated variational circuit grows, complicating verification due to increased circuit complexity. This paper introduces a new protocol to address these challenges and enhance both verifiability and tolerance to channel loss in cloud-based VQAs.

## I. INTRODUCTION

Quantum computation [1] has rapidly transitioned from theoretical speculation to practical application, leveraging the principles of quantum mechanics to tackle problems that are intractable for classical computers. Despite this progress, quantum resources remain scarce and costly, primarily accessible to large corporations. This limitation has spurred efforts to make quantum computation more accessible, especially for clients with limited quantum capabilities.

Blind quantum computation (BQC), a subset of delegated quantum computation (DQC), was first introduced by Childs [2]. It employs quantum one-time padding [3] in gate-based quantum computation (GBQC), enabling a client to delegate quantum computations while ensuring blindness, i.e., the client's input, output, and algorithm remain hidden from the server. Building on this concept, Broadbent et al. [4] proposed the universal blind quantum computation (UBQC) protocol, also known as the BFK protocol. This protocol uses brickwork states as resource states within measurement-based quantum computation (MBQC) [5] on the server side, requiring the client only to prepare a set of qubits  $\left\{ \frac{1}{\sqrt{2}}(|0\rangle + e^{i\phi_k}|1\rangle) \mid \phi_k = \frac{k\pi}{4}, k \in \{0, 1, \dots, 7\} \right\}$  while maintaining blindness. This protocol has spurred research in areas such as verification [6–8], the reduction of the client's quantum capabilities [9–15], joint computational tasks [16], and various applications, including Shor's algorithm [17] and Grover's algorithm [18]. Experimental demonstrations of BQC have also been conducted [19, 20].

In parallel, variational quantum algorithms

(VQAs) [21] have emerged as a promising approach for utilizing noisy intermediate-scale quantum (NISQ) devices to achieve quantum machine learning (QML) [22], demonstrating quantum advantages [23] in areas such as quantum federated learning (QFL) [24], quantum support vector machines (QSVMs) [25], and quantum reinforcement learning (QRL) [26].

Integrating VQAs with BQC provides a promising method for clients with limited quantum capabilities to delegate VQAs to a remote server via cloud networks securely. In previous work, Li et al. [27] combined the BFK protocol [4] with VQAs to implement delegated QFL. However, this approach requires significant quantum resources, with the server needing to entangle  $w \cdot d$  qubits, where  $w$  is the number of qubits required by the original NISQ algorithms and  $d$  is the depth of the brickwork state [4] in the BFK protocol. Wang et al. [28] mitigate this by employing qubit reuse [29], lowering the server's quantum resource consumption to  $2w + 1$  qubits.

Shingu et al.[30] further minimized the server's quantum resource requirements while upholding the principles of BQC by proposing a variational secure cloud quantum computing protocol. This protocol leverages ancilla-driven quantum computation (ADQC)[31] and the no-signaling principle [9] to implement variational quantum algorithms (VQAs) securely. Their approach requires the server to use only  $w + 1$  qubits per operation. However, this protocol lacks verification and is vulnerable to potential malicious operations by the server. Additionally, it is not robust against channel loss, requiring frequent re-delegation as the size of the delegated variational circuit increases, complicating verification. This paper introduces a new protocol that extends their work by incorporating verification and enhancing tolerance to channel loss while maintaining low quantum resource requirements for the server.

The paper is organized as follows: Section II presents the preliminaries, including ADQC, VQAs, and a review

\* bhwang@gdut.edu.cn

† liqin@xtu.edu.cn

of Shingu et al.'s protocol [30]. Section III details the proposed protocol. Section IV analyzes the protocol, focusing on verifiability, blindness, correctness, and comparisons with existing protocols. Section V concludes the paper, discussing potential extensions and suggesting directions for future research.

## II. PRELIMINARIES

### A. Ancilla-Driven Quantum Computation

Ancilla-driven quantum computation (ADQC) [31] is a hybrid model that integrates elements of MBQC and GBQC. In ADQC, an ancillary qubit  $|+\rangle$  couples with a register qubit to implement a single-qubit gate  $J(\phi)$ , where  $J(\phi) = HR_z(\phi)$  and  $\phi$  represents the designated rotation angle, or with two register qubits to implement a controlled-Z gate using a fixed operation such as  $CZ_{RA}(H_R \otimes H_A)$ . Here,  $CZ_{RA}$  denotes the controlled-Z gate between the register and ancillary qubits, with  $H_R$  ( $H_A$ ) representing the Hadamard gate for the register (ancillary) qubit. The ancillary qubit is then measured in a specific basis, consistent with MBQC, to ensure determinism, and the measurement outcome determines the evolution of the register qubit(s), as illustrated in Fig. 1 for  $J(\phi)$  operator.

Ancillary qubits can be realized as optical photons in optical systems [32] and transmitted to distant locations after being coupled to the register qubits, enabling ADQC to be performed remotely by measuring the ancillary qubits in the basis  $\{|\pm\rangle^\phi\} = \left\{ \frac{1}{\sqrt{2}}(|0\rangle \pm e^{i\phi}|1\rangle) \right\}$ .

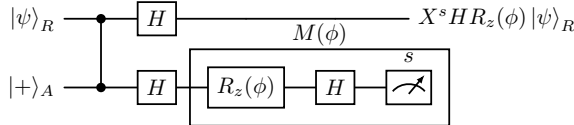


FIG. 1. Circuit for the  $J(\phi)$  operator. The prepared qubits are  $|\psi\rangle_R$  and  $|+\rangle_A$ , where the subscripts  $R$  and  $A$  denote the register qubits and ancillary qubit, respectively. The highlighted section represents the measurement of the ancillary qubit  $|+\rangle_A$  at an angle  $\phi$  in the  $XY$ -plane, i.e., in the basis  $\{|\pm\rangle^\phi\}$ . After measurement, the operation  $X^s HR_z(\phi)$  is obtained, where  $X$  is the Pauli  $X$  operator and  $s$  is the measurement result.

### B. Variational quantum algorithms

Variational quantum algorithms (VQAs) employ parameterized quantum gates, such as  $R_X$ ,  $R_Y$ , and  $R_Z$  [21], to optimize the variational circuit  $|\psi(\vec{\theta})\rangle$ , where  $\psi(\vec{\theta})$  represents a parametrized wave function.

When using classical data in VQAs, encoding techniques such as amplitude encoding [33], angle encoding [34], and hybrid encoding [35] are employed to transform the data into quantum states. The general structure of the circuit is illustrated in Fig. 2. VQA circuits can be conceptualized as quantum neural networks [36], where qubits serve as nodes and quantum gates, represented by matrices, correspond to the weights of a neural network, directly influencing the qubit states.

The structure of the variational circuit is expressed as  $U(\vec{\theta}) = \prod_{i=1}^n U_i(\vec{\theta}^i)$ , where  $\vec{\theta} = \{\theta_1, \theta_2, \dots, \theta_L\}$ . Here, each  $U_i(\vec{\theta}^i)$  represents the  $i$ -th variational layer with its corresponding subset of variational parameters  $\vec{\theta}^i$ . The superscripts  $\{1, \dots, n\}$  denote different variational layers, and the subscripts  $\{1, \dots, L\}$  refer to specific variational parameters within the entire set  $\vec{\theta}$ .

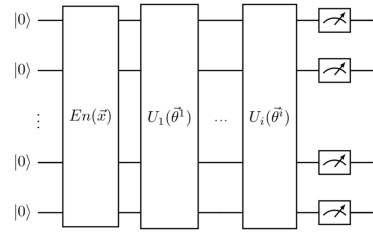


FIG. 2. General variational quantum circuit, where all qubits are initialized in the state  $|0\rangle$ . The operator  $En$  encodes classical data  $\vec{x}$  into quantum state  $En(\vec{x})|0\rangle^{\otimes w}$ , and  $U(\vec{\theta}) = \prod_{i=1}^n U_i(\vec{\theta}^i)$  represents a variational layer with a specific ansatz.

The variational parameters  $\vec{\theta}$  in VQAs are iteratively updated and optimized by a classical optimizer, such as Adam [37], utilizing measurement outcomes from the quantum circuit in conjunction with the cost function:

$$\begin{aligned} C(\vec{\theta}) &= f(E(\vec{\theta})) \\ &= f(\langle \psi(\vec{\theta}) | O | \psi(\vec{\theta}) \rangle), \end{aligned} \quad (1)$$

where  $E(\vec{\theta})$  represents the expectation value of the output state  $|\psi(\vec{\theta})\rangle$  for a given set of parameters  $\vec{\theta}$ , and  $O$  is the measurement observable.

The parameters  $\vec{\theta} = \{\theta_j\}_{j=1}^L$  are iteratively updated via gradient descent, such that  $\vec{\theta} \leftarrow \vec{\theta} - \eta \nabla C(\vec{\theta})$ , where  $\eta$  denotes the learning rate. The gradients  $\nabla C(\vec{\theta}) = \{\nabla C(\theta_j)\}_{j=1}^L$  are computed using the parameter-shift rule [38]. Specifically, the gradient  $\nabla C(\theta_j)$  is given by:

$$\begin{aligned} \nabla C(\theta_j) &= \frac{1}{2} \left[ C\left(\theta_j + \frac{\pi}{2}\right) - C\left(\theta_j - \frac{\pi}{2}\right) \right] \\ &= \frac{1}{2} \left[ f\left(E\left(\theta_j + \frac{\pi}{2}\right)\right) - f\left(E\left(\theta_j - \frac{\pi}{2}\right)\right) \right], \end{aligned} \quad (2)$$

where  $\theta_j \pm \frac{\pi}{2} = \{\theta_1 \dots \theta_{j \pm \frac{\pi}{2}} \dots \theta_L\}$ .

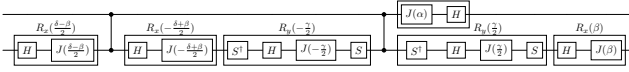


FIG. 3. Circuit for the wo-qubit control gates. The server interacts with the client to obtain 6  $J(\phi)$  operators with parameters  $\alpha, \beta, \gamma$ , and  $\delta$ .

### C. Review of Shingu et al.'s protocol

The variational secure cloud quantum computing protocol proposed by Shingu et al. employs the circuit depicted in Fig. 1 and necessitates additional gates to execute two-qubit control operations, as shown in Fig. 3.

Specifically, a single-qubit gate is implemented using three consecutive  $J(\phi)$  operators. In contrast, a two-qubit controlled gate requires the server to perform  $CZ$  gates,  $H$  gates, and two phase gates: the  $S$  gate and the  $S^\dagger$  gate. The client receives and measures ancillary qubits sent by the server to evolve the register qubits according to ADQC. Subsequently, the server measures the output register qubits and communicates the results to the client.

The protocol proceeds as follows:

#### A1 (Preparation phase):

1. The server publicly announces the following: the number of original and variational quantum circuits for gradient calculations,  $G$ ; the set of unitary operators  $\{U_{AN}^{(c)}\}_{c=1}^G$ , where  $c$  denotes the  $c$ -th circuit; the set of measurement observables  $\{\hat{A}_1^{(c)}, \hat{A}_2^{(c)}, \dots, \hat{A}_{K^{(c)}}^{(c)}\}_{c=1}^G$ , where  $K^{(c)}$  is the number of observables measured in the  $c$ -th circuit; the number of circuit repetitions  $\{\mathcal{R}^{(c)}\}_{c=1}^G$ ; the initial states  $\{|\psi_{out}^{(c)}(\vec{\theta}[0])\rangle\}_{c=1}^G$ , where  $\vec{\theta}[0]$  indicates the initial parameters at the current iteration step; the number of variational parameters,  $L$ ; and the total number of iteration steps for VQAs,  $\mathcal{I}$ .
2. The server prepares  $w$  register qubits  $|0\rangle_R$  and one ancillary qubit  $|+\rangle_A$ .

#### A2 (Computation phase):

1. Adopt the quantum circuits  $\{U_{AN}^{(c)}\}_{c=1}^G$  using the circuits depicted in Fig. 1 and Fig. 3 to generate the trial wave functions  $\left\{|\psi^{(c)}(\vec{\theta}[1])\rangle\right\}_{c=1}^G$ .
2. The server measures the output register qubits' states with  $\{\hat{A}_1^{(c)}, \hat{A}_2^{(c)}, \dots, \hat{A}_{K^{(c)}}^{(c)}\}_{c=1}^G$  and sends the results to the client via classical communication.
3. The server reprepares ancillary qubit  $|+\rangle_A$ .
4. The client compensates for the Pauli byproduct effect.

#### A3 (Parameters updating phase):

1. The server and the client repeat **A2**  $\{\mathcal{R}^{(c)}\}_{c=1}^G$  times to derive the expectation values of  $\{\hat{A}_1^{(c)}, \hat{A}_2^{(c)}, \dots, \hat{A}_{K^{(c)}}^{(c)}\}_{c=1}^G$ .
2. The client updates the parameters using its optimizer, such as the parameter-shift rule (Eq. 2), yielding  $\vec{\theta}[2] = (\theta_1[2], \dots, \theta_L[2])^T$  for the next step.
3. The client computes the measurement angles for adopting circuits  $\{U_{AN}^{(c)}\}_{c=1}^G$  with  $\vec{\theta}[2]$ .
4. The client and server reiterate the above steps  $(\mathcal{I} - 2)$  times with  $\{U_{AN}^{(c)}\}_{c=1}^G$  and  $\vec{\theta}[j]$ . Based on the results from the  $j$ -th step, classical computations update the client's parameters to  $\vec{\theta}[j + 1]$  for  $j = 2, 3, \dots, \mathcal{I} - 1$ .

This protocol enables the delegation of VQAs through interaction between the server and the client, requiring only  $w$  register qubits and a single ancillary qubit. However, if any of the coupled ancillary qubits are lost during transmission, the circuit needs to be re-delegated, which results in a low tolerance to channel loss. Even the most efficient single-photon detectors in optics, which have shown 99% efficiency in recent studies [39, 40], are not immune to this issue. For sufficiently large circuits, the probability of re-delegation becomes significant. For example, consider a circuit where each block consists of an average of four single-qubit gates and one two-qubit control gate. A circuit with six blocks would require  $4 \times 3 \times 6 + 1 \times 6 \times 6 = 108$   $J(\phi)$  operators. The probability of needing to re-delegate the circuit is approximately  $(1 - 0.99^{108}) \approx 66.22\%$  per delegated  $J(\phi)$  operator, increasing exponentially with the number of  $J(\phi)$  operators.

Due to channel loss, adding dummy gates for verification becomes impractical, as the circuit would require enough extra trap wires for dummy gates without affecting the wires used for computation. This increases the circuit size and leads to frequent circuit re-delegation. One potential solution to mitigate channel loss is to share Bell pairs between the server and the client, with repeated entanglement generation until successful [9]. However, in each delegation of the  $J(\phi)$  operator, as illustrated in Fig. 1, the ancillary qubit is sent to the client after coupling with the register qubit. While the server can send one half of the Bell pair to the client for measurement, further measurements on the remaining half are required on the server side after coupling with the register qubit. The server cannot complete these measurements in Fig. 1, rendering the use of Bell pairs ineffective in this context.

### III. THE PROPOSED PROTOCOL

We adopt the strategy outlined in [41], where the server performs measurements after coupling the an-

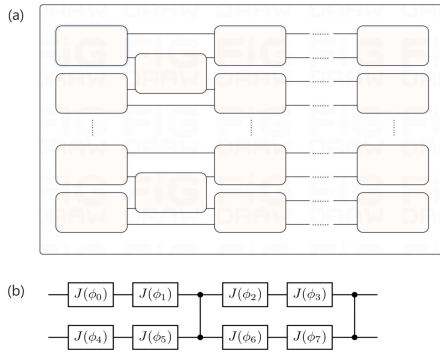


FIG. 4. (a) The gate pattern circuit, which includes 8  $J(\phi)$  operators and 2  $CZ$  gates. (b) The universal gate patterns, which are composed of multiple blocks, each block representing a gate pattern.

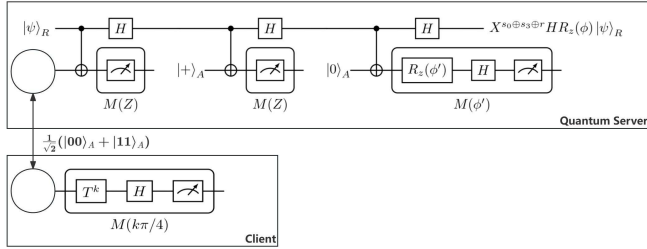


FIG. 5. Realization of the  $J(\phi)$  operator: The server sends one qubit from a Bell pair to the client, who then applies a  $T$  gate  $k$  times, where  $k$  is randomly and uniformly selected from  $\{0, 1, \dots, 7\}$ , followed by a Hadamard gate  $H$ , and measures in the  $Z$  basis. This measurement is equivalent to measuring in the basis  $\{|\pm\rangle^{k\pi/4}\}$ . The server then performs a sequence of operations on the ancillary and register qubits, including a fixed coupling operation  $CX_{RA}(H_R \otimes I_A)$ , where  $CX$  is the controlled-X gate and  $I$  is the identity gate, followed by measurements on the ancillary qubits.

illary qubits with the register qubits, effectively addressing the limitations of using Bell pairs to tolerate channel loss in Shingu et al.'s protocol. The client is required to perform measurements in the bases  $\{|\pm\rangle^{\phi_k} \mid \phi_k = \frac{k\pi}{4}, k \in \{0, 1, \dots, 7\}\}$ . For verification, we use trap qubits to create dummy gates in the trap wires as the circuit is transformed into the universal gate patterns shown in Fig. 4. Additionally, we delegate encrypted measurements of the output register qubits to the server, making it difficult to identify the trap wires in the circuits.

The client delegates the  $J(\phi)$  operators within the universal gate patterns shown in Fig. 5, while the server provides the  $CZ$  gates. This process includes preparation, computation, verification, and parameter updating phases, as briefly illustrated in Fig. 6. The specific steps are as follows:

### B1 (Preparation phase):

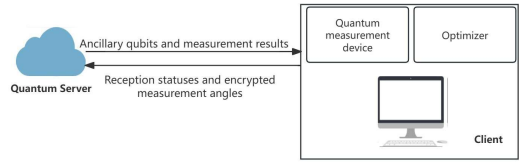


FIG. 6. Brief process of the proposed protocol: The server sends an ancillary qubit, as one half of a Bell pair, to the client, who measures it in the basis  $\{|\pm\rangle^{\frac{k\pi}{4}}\}$ . The client then sends the reception status back to the server, requesting a resend if the qubit is lost. The server performs encrypted measurements as instructed by the client and returns the results, enabling the client to verify the server's honesty and calculate encrypted measurement angles and gradients for the optimizer.

1. The server publicly announces the following: the number of original and variant variational quantum circuits for gradient calculation,  $G$ ; the set of transformed unitary operators,  $\{U_{AN}^{(c)}\}_{c=1}^G$ ; the number of circuit repetitions,  $\{\mathcal{R}^{(c)}\}_{c=1}^G$ ; the initial states,  $\{|\psi_{out}^{(c)}(\vec{\theta}[0])\rangle\}_{c=1}^G$ , for the  $G$  circuits; the number of variational parameters,  $L$ ; the total number of iteration steps for VQAs,  $\mathcal{I}$ ; and the size of the transformed circuits,  $\{N \times M\}_{c=1}^G$ , where  $N = 3w$  and  $M$  represent the number of input qubits and the circuit depth, respectively.
2. The server prepares  $N$  register qubits  $|0\rangle_R$ , two ancillary qubits  $\frac{1}{\sqrt{2}}(|00\rangle_A + |11\rangle_A)$  as a Bell pair, one ancillary qubit  $|+\rangle_A$ , and one ancillary qubit  $|0\rangle_A$ . Meanwhile, the client chooses  $\frac{2N}{3}$  register qubits as trap qubits for verification, which is optimal [6].

### B2 (Computation phase):

1. The server sends one qubit from the Bell pair to the client, who measures it in the basis  $\{|\pm\rangle^{\frac{k\pi}{4}}\}$ , yielding the result  $s_0$ , where  $k$  is randomly and uniformly selected from  $\{0, 1, \dots, 7\}$ . The client generates a random bit  $r$  to indicate the reception status, setting it to 0 if the particle arrived successfully or to 1 if it was lost. This status is communicated to the server, who generates a new Bell pair and resends half of it to the client until the qubit arrives successfully. The other half of the Bell pair will eventually be in the state  $Z^{s_0} |+\rangle_A^{\frac{k\pi}{4}}$ .
2. The server employs the transformed circuits  $\{U_{AN}^{(c)}\}_{c=1}^G$  using the  $J(\phi)$  operator, as depicted in Fig. 5, to generate the trial wave functions  $\{|\psi^{(c)}(\vec{\theta}[1])\rangle\}_{c=1}^G$ . In each delegation of the  $J(\phi)$  operator, the  $Z$  measurement results  $s_1$  and  $s_2$  are first sent to the client. The client then uses  $s_1$  to compute the encrypted measurement angle  $\phi' = \phi - (-1)^{s_1} \left(\frac{k\pi}{4}\right) + (r + s_0)\pi$ , where  $r \in \{0, 1\}$  is

a random bit chosen by the client. This encrypted angle  $\phi'$  is sent to the server, which measures in the basis  $\{|\pm\rangle^{\phi'}\}$ . The resulting measurement outcome  $s_3$  is then sent to the client. The actual measurement angle  $\phi$  is adaptively chosen based on prior Pauli byproducts to ensure determinism in MBQC.

3. In each transformed circuit, a random selection of  $\frac{2N}{3}$  wires is designated as trap wires, where dummy gates are implemented. On half of these trap wires, the identity gate is applied  $M$  times on each wire. On the remaining trap wires, a single Hadamard gate is randomly inserted, with the identity gate occupying the other  $M - 1$  positions on each wire.
4. The server measures the output register qubits using the encrypted measurement angle  $\phi'_{\text{out}}$  provided by the client, where  $\phi'_{\text{out}} = (-1)^{x_{\text{out}}}\phi_{\text{out}} + z_{\text{out}}\pi$ , with  $\phi_{\text{out}}$  being the actual measurement angle. The measurement results are then sent to the client. The client sets  $\phi_{\text{out}}$  to select the desired measurement basis in the  $XY$ -plane. To measure in the  $Z$  basis, the client delegates an additional  $R_y(\frac{\pi}{2})$  gate at the end of the circuit and sets  $\phi_{\text{out}} = \pi$ .
5. The server resets one ancillary qubit to  $|+\rangle_A$ , one to  $|0\rangle_A$ , and reprepares Bell pair  $\frac{1}{\sqrt{2}}(|00\rangle_A + |11\rangle_A)$ .
6. The client compensates for the Pauli byproduct effect by flipping the measurement result of the output register qubits.

### B3 (Verification phase):

1. At the end of **B2(3)**, the output register qubits consist of non-trap qubits and trap qubits in a random permutation designed by the client. The output state can be written as  $\sigma_q P |\Psi\rangle_R = \sigma_q P \left( |\psi\rangle_{\text{out}}^{\frac{N}{3}} \otimes |0\rangle_T^{\frac{N}{3}} \otimes |+\rangle_T^{\frac{N}{3}} \right)$ , where  $|\psi\rangle_{\text{out}}$  represents the non-trap qubits, and  $\sigma_q$  is the Pauli byproduct operator. The subscript  $R$  includes both non-trap qubits ( $\text{out}$ ) and trap qubits ( $T$ ), with  $P$  as the permutation.
2. The client instructs the server to measure all desired trap qubits,  $|0\rangle_T^{\frac{N}{3}}$  in the  $Z$  basis and  $|+\rangle_T^{\frac{N}{3}}$  in the  $X$  basis, in **B2(4)**. If any undesired output  $|1\rangle_T$  in the  $Z$  basis or  $|-\rangle_T$  in the  $X$  basis is obtained after compensating for the Pauli byproduct effect, the protocol is terminated.

### B4 (Parameters updating phase):

1. The server and the client repeat **B2** to **B3**  $\{\mathcal{R}^{(c)}\}_{c=1}^G$  times to derive the expectation values of  $\{\hat{A}_1^{(c)}, \hat{A}_2^{(c)}, \dots, \hat{A}_{K^{(c)}}^{(c)}\}_{c=1}^G$ .
2. The client computes the measurement angles for adopting circuits  $\{U_{\text{AN}}^{(c)}\}_{c=1}^G$  with  $\vec{\theta}[2]$ .

3. The client utilizes its optimizer to update the parameters, resulting in  $\vec{\theta}[2] = (\theta_1[2], \dots, \theta_L[2])^T$  for the next step.
4. The client and server reiterate the above steps  $(\mathcal{I} - 2)$  times with  $\{U_{\text{AN}}^{(c)}\}_{c=1}^G$  and  $\vec{\theta}[j]$ . Based on the results from the  $j$ -th step, classical computations update the client's parameters to  $\vec{\theta}[j + 1]$  for  $j = 2, 3, \dots, \mathcal{I} - 1$ .

## IV. ANALYSIS

### A. Verifiability

We use trap qubits to detect malicious operations on the output register qubits. The verifiability of the proposed protocol is demonstrated in Theorem I, which follows a method similar to that in [6], where further details can be found.

**Theorem 1:** The probability of the client being tricked by the server is exponentially small.

*Proof.* If the server is malicious, it may deviate from the state  $\rho = \sigma_q |\Psi\rangle_R \langle \Psi|_R \sigma_q^\dagger$  to any other state. However, due to the completely-positive-trace-preserving (CPTP) map [11], this deviation can be detected as a random Pauli attack.

Suppose  $\sigma_\alpha$  represents a random Pauli attack, where the weight of  $\sigma_\alpha (|\alpha|)$  is the number of non-trivial operators in  $\sigma_\alpha$ , such that  $|\alpha| = a + b + c$ , where  $a$ ,  $b$ , and  $c$  are the numbers of  $X$ ,  $Z$ , and  $XZ$  operators in  $\sigma_\alpha$ , respectively. We have  $|\alpha| = a + b + c \leq 3 \max(a, b, c)$ . When these operators are applied to the output trap qubits  $|0\rangle_T$  and  $|+\rangle_T$ ,  $X$  will only change  $|0\rangle_T$  to  $|1\rangle_T$ ,  $Z$  will only change  $|+\rangle_T$  to  $|-\rangle_T$ , and  $XZ$  will change both  $|0\rangle_T$  and  $|+\rangle_T$  to  $|1\rangle_T$  and  $|-\rangle_T$ , respectively.

We can calculate the probabilities that each operator in  $\sigma_\alpha$  does not change any trap qubits. Suppose  $\max(a, b, c) = a$ . An  $X$  operator that does not change any trap qubits will only act on  $|+\rangle_T$  and non-trap qubits, the number of which is  $\frac{2N}{3}$ . Thus, the probability is:

$$\begin{aligned} \frac{C(\frac{2N}{3}, a)}{C(N, a)} &= \left(\frac{2}{3}\right)^a \frac{\prod_{k=0}^{a-1} (N - \frac{3}{2}k)}{\prod_{k=0}^{a-1} (N - k)} \\ &\leq \left(\frac{2}{3}\right)^a \leq \left(\frac{2}{3}\right)^{\frac{|\alpha|}{3}}. \end{aligned} \quad (3)$$

Similarly, for  $\max(a, b, c) = b$ , the probability  $\frac{C(\frac{2N}{3}, b)}{C(N, b)} \leq \left(\frac{2}{3}\right)^{\frac{|\alpha|}{3}}$ , and for  $\max(a, b, c) = c$ , the probability  $\frac{C(\frac{N}{3}, c)}{C(N, c)} \leq \left(\frac{1}{3}\right)^{\frac{|\alpha|}{3}}$  can be calculated in the same way.

The proposed protocol requires the client to send qubits, qubit reception statuses, and encrypted measurement angles, which violates the no-signaling principle. However, the permutation  $P$  is not included in these

transmissions, ensuring  $P$  remains secret. By encrypting the measurement angles for the trap qubits after the circuit construction is completed, the server cannot distinguish between trap and non-trap qubits, further protecting  $P$ .

After the client randomly selects a permutation  $P$ , the probability that  $P^\dagger \sigma_\alpha P$  does not alter any trap qubits is at most  $(\frac{2}{3})^{\frac{|\alpha|}{3}}$ . Consequently, the probability that the client is deceived by the server is at most  $\prod_{c=1}^G (\frac{2}{3})^{\frac{|\mathcal{R}^{(c)}| |\alpha|}{3}} = (\frac{2}{3})^{\frac{\sum_{c=1}^G |\mathcal{R}^{(c)}| |\alpha|}{3}}$ , where  $G$  is the number of original and variant quantum circuits used to calculate gradients, and  $\{\mathcal{R}^{(c)}\}_{c=1}^G$  is the set of circuit repetitions. This probability becomes exponentially small when  $\sum_{c=1}^G |\mathcal{R}^{(c)}|$  is sufficiently large, ensuring the protocol's verifiability.  $\square$

## B. Blindness and Correctness

We utilize universal gate patterns in the proposed protocol to ensure both blindness and correctness during computation, with minimal information leakage. Specifically, only the size of the delegated circuit, corresponding to the size of the universal gate patterns, is revealed. The following theorems establish the blindness and correctness of the proposed protocol in the context of cloud-based VQAs.

**Theorem 2:** The proposed protocol guarantees input, output, and algorithm blindness.

*Proof. Input Blindness:* After the client measures one qubit of the Bell pair, the remaining qubit is left in a maximally mixed state,  $\frac{1}{16} \sum_{s_0=0}^1 \sum_{k=0}^7 (Z^{s_0} |+\rangle_A^{\frac{k\pi}{4}} \langle +|_A^{\frac{k\pi}{4}} Z^{s_0\dagger}) = \frac{I}{2}$ , with the value of  $k$  hidden from the server.

**Output Blindness:** After applying the  $J(\phi)$  operator, the register qubit is  $X^{s_0 \oplus s_3 \oplus r} H R_z(\phi) |\psi\rangle_R$ . Upon completion of the delegated circuit, the output register qubits are  $X^{x_{out}} Z^{z_{out}} U |\Psi\rangle_R$ , where  $X^{x_{out}} Z^{z_{out}}$  are Pauli byproducts. Since the server cannot determine  $r$  and  $s_0$ , it cannot compensate for  $X^{s_0 \oplus s_3 \oplus r}$ , and therefore cannot compensate for  $X^{x_{out}} Z^{z_{out}}$ , leaving the output qubits in a maximally mixed state.

**Algorithm Blindness:** When the client sends the encrypted measurement angle  $\phi' = \phi - (-1)^{s_1} \frac{k\pi}{4} + (s_0 + r)\pi$  to the server, the true measurement angle  $\phi$  remains hidden from the server, as  $k$  and  $r$  are randomly chosen, and  $s_0$  is never disclosed to the server.

Therefore, the server can only deduce the general structure of the universal gate patterns.  $\square$

**Theorem 3:** The proposed protocol ensures correctness throughout the computation.

*Proof.* In each gate pattern, as illustrated in Fig. 4(a), the server directly applies the  $CZ$  gate, while the  $J(\phi)$  opera-

tor is realized using the circuit shown in Fig. 5 from [41], resulting in  $H R_z(\phi) |\psi\rangle_R$  with Pauli byproducts. The client adjusts the measurement results sent by the server based on these Pauli byproducts, ensuring the correct  $J(\phi)$  operators in the universal gate patterns.

Arbitrary single-qubit gates can be implemented within this gate pattern. For two arbitrary single-qubit gates  $U_1$  and  $U_2$ , we decompose  $U_1$  as  $R_z(\phi_0) R_x(\phi_1) R_z(\phi_2)$  and  $U_2$  as  $R_z(\phi_4) R_x(\phi_5) R_z(\phi_6)$  using Euler's rotation theorem [42]. This can be realized in the gate pattern as follows:

$$U_1 \otimes U_2 = (J_1(\phi_0) J_1(\phi_1)) \otimes (J_2(\phi_4) J_2(\phi_5 = 0)) CZ_{12} \\ (J_1(\phi_2) J_1(\phi_3)) \otimes (J_2(\phi_6) J_2(\phi_7 = 0)) CZ_{12}. \quad (4)$$

The  $CX$  gate can also be implemented within this pattern:

$$CX_{12} = (J_1(\phi_0 = 0) J_1(\phi_1 = 0)) \otimes \\ (J_2(\phi_4 = 0) J_2(\phi_5 = \frac{\pi}{4})) CZ_{12} \\ (J_1(\phi_2 = \frac{\pi}{4}) J_1(\phi_3 = 0)) \otimes \\ (J_2(\phi_6 = 0) J_2(\phi_7 = -\frac{\pi}{4})) CZ_{12}. \quad (5)$$

Using these gates, we can realize any quantum gates in VQAs. Additionally, the delegated computation adheres to the rules of MBQC, where measurement angles are adaptively chosen to move all Pauli byproducts to the leftmost position, resulting in  $X^{x_{out}} Z^{z_{out}} U |\Psi\rangle_R$ . By appropriately correcting the measurement results, the client ultimately obtains the desired state  $U |\psi\rangle_{out}$ .  $\square$

## C. Comparisons

Table I compares the proposed protocol with related protocols for cloud-based VQAs. Our protocol builds upon the method introduced by Shingu et al. [30], incorporating verification to enhance robustness while maintaining low quantum resource requirements. Notably, our protocol requires measurements in specific bases.

An additional advantage of our protocol is its improved tolerance to channel loss. In Shingu et al.'s protocol, the loss of any ancillary qubit during transmission necessitates re-delegating the entire circuit, which is particularly problematic for large circuits. Our protocol, however, allows the server to perform encrypted measurements, achieving tolerance by sharing Bell pairs between the server and client. While both Wang et al.'s [28] and Li et al.'s [27] BFK-based protocols also tolerate channel loss, Wang et al.'s protocol requires  $6w \cdot d$  qubits with verification, and Li et al.'s protocol requires  $6w + 1$  qubits with verification, where  $w$  is the number of qubits in the

TABLE I. Comparison among different protocols for cloud-based VQAs.

	Verifiable	Client's quantum capabilities	Tolerance to channel loss	Server's resource consumption
Li et al.'s BFK-based protocol [27]	Yes	Prepare qubits	Yes	$6w \cdot d$
Wang et al.'s BFK-based protocol [28]	Yes	Measure qubits	Yes	$6w + 1$
Shingu et al.'s protocol [30]	No	Measure qubits	No	$w + 1$
The proposed protocol	Yes	Measure qubits	Yes	$3w + 4$

original NISQ algorithms, and  $d$  is the depth of the brickwork state in the BFK protocol. In contrast, our protocol, adapted from Shingu et al.'s approach, requires only  $3w$  register qubits and four ancillary qubits. While our protocol employs more qubits due to the added verification step, it still uses significantly fewer qubits than the BFK-based protocols.

## V. CONCLUSION AND DISCUSSION

In this paper, we propose a protocol for cloud-based VQAs that builds upon the work of Shingu et al., enhancing both verifiability and tolerance to channel loss. We have also demonstrated the blindness and correctness of the protocol, ensuring security and accuracy in cloud-based VQAs. Additionally, we compare the client's quantum capability requirements and the server's resource consumption with those in Shingu et al.'s protocol and the BFK-based protocols.

The proposed protocol can be further extended through two potential schemes. First, if the client possesses multiple photon detectors, the  $J(\phi)$  operators can be performed on multiple register qubits in parallel,

thereby accelerating the protocol's runtime. However, this approach would increase the ancillary qubit resource consumption. Second, the protocol can be adapted for clients without quantum capabilities by employing the double-server blind quantum computation method [11], which is compatible with the proposed protocol.

Further research is necessary in several areas. Reducing communication costs while ensuring security remains a significant challenge. Additionally, exploring alternative verification methods to reduce quantum resource consumption further would be beneficial. Lastly, instead of directly transforming parameterized gate-based quantum circuits into MBQC patterns, adopting an MBQC-native approach [43–45] for VQAs could offer improved circuit depth reduction, making it suitable for adaptation to cloud-based VQAs. Our protocol has the potential to pave the way for real-world applications of cloud-based quantum machine learning.

## ACKNOWLEDGMENTS

This work is supported by the National Natural Science Foundation of China under Grant Nos. 62072119 and 62271436.

---

[1] D. P. DiVincenzo, *Science* **270**, 255 (1995).  
[2] A. M. Childs, *Quantum Information & Computation* **5**, 456 (2005).  
[3] F.-G. Deng and G. L. Long, *Physical Review A* **69**, 052319 (2004).  
[4] A. Broadbent, J. Fitzsimons, and E. Kashefi, in *2009 50th Annual IEEE Symposium on Foundations of Computer Science* (IEEE, 2009) pp. 517–526.  
[5] H. J. Briegel, D. E. Browne, W. Dür, R. Raussendorf, and M. Van den Nest, *Nature Physics* **5**, 19 (2009).  
[6] T. Morimae, *Physical Review A* **89**, 060302(R) (2014).  
[7] J. F. Fitzsimons and E. Kashefi, *Physical Review A* **96**, 012303 (2017).  
[8] S. Barz, J. F. Fitzsimons, E. Kashefi, and P. Walther, *Nature physics* **9**, 727 (2013).  
[9] T. Morimae and K. Fujii, *Physical Review A* **87**, 050301(R) (2013).  
[10] Q. Li, C. Liu, Y. Peng, F. Yu, and C. Zhang, *Optics & Laser Technology* **142**, 107190 (2021).  
[11] T. Morimae and K. Fujii, *Physical Review Letters* **111**, 020502 (2013).  
[12] Q. Li, W. H. Chan, C. Wu, and Z. Wen, *Physical Review A* **89**, 040302(R) (2014).  
[13] H.-R. Xu and B.-H. Wang, *Laser Physics Letters* **19**, 015202 (2021).  
[14] X. Zhang, *Quantum Information Processing* **21**, 14 (2022).  
[15] S. Cao, *New Journal of Physics* **25**, 103028 (2023).  
[16] F. Sciarrino, B. Polacchi, D. Leichtle, L. Limongi, G. Carvacho, G. Milani, N. Spagnolo, M. Kaplan, and E. Kashefi, *Nature Communications* (2023).  
[17] A. Das and B. C. Sanders, *Physical Review A* **106**, 012421 (2022).  
[18] C. Gustiani and D. P. DiVincenzo, *Physical Review A* **104**, 062422 (2021).  
[19] S. Barz, E. Kashefi, A. Broadbent, J. F. Fitzsimons,

A. Zeilinger, and P. Walther, *science* **335**, 303 (2012).

[20] H.-L. Huang, Q. Zhao, X. Ma, C. Liu, Z.-E. Su, X.-L. Wang, L. Li, N.-L. Liu, B. C. Sanders, C.-Y. Lu, and J.-W. Pan, *Physical Review Letters* **119**, 050503 (2017).

[21] M. Cerezo, A. Arrasmith, R. Babbush, S. C. Benjamin, S. Endo, K. Fujii, J. R. McClean, K. Mitarai, X. Yuan, L. Cincio, *et al.*, *Nature Reviews Physics* **3**, 625 (2021).

[22] J. Biamonte, P. Wittek, N. Pancotti, P. Rebentrost, N. Wiebe, and S. Lloyd, *Nature* **549**, 195 (2017).

[23] T. M. Khan and A. Robles-Kelly, *IEEE Access* **8**, 219275 (2020).

[24] S. Y.-C. Chen and S. Yoo, *Entropy* **23**, 460 (2021).

[25] P. Rebentrost, M. Mohseni, and S. Lloyd, *Physical Review Letters* **113**, 130503 (2014).

[26] D. Dong, C. Chen, H. Li, and T.-J. Tarn, *IEEE Transactions on Systems, Man, and Cybernetics, Part B (Cybernetics)* **38**, 1207 (2008).

[27] W. Li, S. Lu, and D.-L. Deng, *Science China Physics, Mechanics & Astronomy* **64**, 100312 (2021).

[28] Y. Wang, J. Quan, and Q. Li, in *2022 14th International Conference on Wireless Communications and Signal Processing (WCSP)* (IEEE, 2022) pp. 804–808.

[29] M. Houshmand, M. Houshmand, and J. F. Fitzsimons, *Physical Review A* **98**, 012318 (2018).

[30] Y. Shingu, Y. Takeuchi, S. Endo, S. Kawabata, S. Watabe, T. Nikuni, H. Hakoshima, and Y. Matsuzaki, *Physical Review A* **105**, 022603 (2022).

[31] J. Anders, D. K. L. Oi, E. Kashefi, D. E. Browne, and E. Andersson, *Physical Review A* **82**, 020301(R) (2010).

[32] G. S. Agarwal, *Quantum optics* (Cambridge University Press, 2012).

[33] K. Nakaji, S. Uno, Y. Suzuki, R. Raymond, T. Onodera, T. Tanaka, H. Tezuka, N. Mitsuda, and N. Yamamoto, *Phys. Rev. Res.* **4**, 023136 (2022).

[34] M. Weigold, J. Barzen, F. Leymann, and M. Salm, in *Proceedings of the 27th Conference on Pattern Languages of Programs* (2020) pp. 1–11.

[35] B. Bhabhatsatam and S. Smachat, in *2023 20th International Joint Conference on Computer Science and Software Engineering (JCSSE)* (2023) pp. 512–516.

[36] S. Jeswal and S. Chakraverty, *Archives of Computational Methods in Engineering* **26**, 793 (2019).

[37] D. Kingma and J. Ba, in *International Conference on Learning Representations (ICLR)* (San Diego, CA, USA, 2015).

[38] M. Schuld, V. Bergholm, C. Gogolin, J. Izaac, and N. Killoran, *Physical Review A* **99**, 032331 (2019).

[39] A. Kuzanyan, A. Kuzanyan, and V. Nikoghosyan, *Journal of Contemporary Physics (Armenian Academy of Sciences)* **53**, 338 (2018).

[40] J. Wenner, Y. Yin, Y. Chen, R. Barends, B. Chiaro, E. Jeffrey, J. Kelly, A. Megrant, J. Y. Mutus, C. Neill, P. J. J. O’Malley, P. Roushan, D. Sank, A. Vainsencher, T. C. White, A. N. Korotkov, A. N. Cleland, and J. M. Martinis, *Physical Review Letters* **112**, 210501 (2014).

[41] T. Sueki, T. Koshiba, and T. Morimae, *Physical Review A* **87**, 060301(R) (2013).

[42] P. Gothen and A. Guedes de Oliveira, *The College Mathematics Journal* **54**, 171 (2023).

[43] A. Schroeder, M. Heller, and M. Gachechiladze, *New Journal of Physics* (2023).

[44] A. Chan, Z. Shi, L. Dellantonio, W. Dür, and C. A. Muschik, *Physical Review Letters* **132**, 240601 (2024).

[45] L. M. Calderón, P. Feldmann, R. Raussendorf, and D. Bondarenko, arXiv preprint arXiv:2405.08319 (2024).